Published in final edited form as:
Exp Eye Res. 2013 May ; 110: 96–106. doi:10.1016/j.exer.2013.03.003.

Specific sphingolipid content decrease in *Cerkl* knockdown mouse retinas

Alejandro Garanto[a,b,c,1], **Nawajes A. Mandal**[d,e], **Meritxell Egido-Gabás**[f], **Gemma Marfany**[a,b,c], **Gemma Fabriàs**[f], **Robert E. Anderson**[d,e,g], **Josefina Casas**[f], and **Roser Gonzàlez-Duarte**[a,b,c,*]

[a]Departament de Genètica, Facultat de Biologia, Universitat de Barcelona, Barcelona, Spain

[b]Institut de Biomedicina (IBUB), Universitat de Barcelona, Barcelona, Spain

[c]CIBERER, Instituto de Salud Carlos III, Barcelona, Spain

[d]Dean McGee Eye Institute, Oklahoma City, USA

[e]Department of Ophthalmology, University of Oklahoma Health Sciences Center, Oklahoma City, USA

[f]Research Unit on BioActive Molecules (RUBAM), Departamento de Química BioMédica, Instituto de Química Avanzada de Catalunya IQAC-CSIC, Barcelona, Spain

[g]Department of Cell Biology, University of Oklahoma Health Sciences Center, Oklahoma City, USA

Abstract

Sphingolipids (SPLs) are finely tuned structural compounds and bioactive molecules involved in membrane fluidity and cellular homeostasis. The core sphingolipid, ceramide (CER), and its derivatives, regulate several crucial processes in neuronal cells, among them cell differentiation, cell–cell interactions, membrane conductance, synaptic transmission, and apoptosis. Mutations in *Ceramide Kinase-Like* (*CERKL*) cause autosomal recessive Retinitis Pigmentosa and Cone Rod Dystrophy. The presence of a conserved lipid kinase domain and the overall similarity with CERK suggested that CERKL might play a role in the SPL metabolism as a CER kinase. Unfortunately, CERKL function and substrate(s), as well as its contribution to the retinal etiopathology, remain as yet unknown. In this work we aimed to characterize the mouse retinal sphingolipidome by UPLC-TOF to first, thoroughly investigate the SPL composition of the murine retina, compare it to our *Cerkl* −/− model, and finally assess new possible CERKL substrates by phosphorus quantification and protein-lipid overlay. Our results showed a consistent and notable decrease of the retinal SPL content (mainly ranging from 30% to 60%) in the *Cerkl* −/− compared to WT retinas, which was particularly evident in the glucosyl/galactosyl ceramide species (Glc/GalCer) whereas the

*Corresponding author. Universitat de Barcelona, Departament de Genètica, Avda. Diagonal 643, 08028 Barcelona, Spain. Tel.: +34 934021034. rgonzalez@ub.edu (R. Gonzàlez-Duarte).
[1]Present address: Department of Human Genetics, Radboud University Nijmegen Medical Centre, Nijmegen, The Netherlands.

Appendix A. Supplementary data: Supplementary data related to this article can be found at http://dx.doi.org/10.1016/j.exer.2013.03.003.

phospholipids and neutral lipids remained unaltered. Moreover, evidence in favor of CERKL binding to GlcCer, GalCer and sphingomyelin has been gathered. Altogether, these results highlight the involvement of CERKL in the SPL metabolism, question its role as a kinase, and open new scenarios concerning its function.

Keywords

knockout models; retinal dystrophy; sphingolipid

1. Introduction

Sphingolipids (SPLs) are a group of membrane lipids involved in several cellular key processes. In the last decades, several roles including regulatory functions have been assigned to SPLs, revealing that they far surpass being mere structural components, as they play crucial roles on cell cycle control, immunological response, autophagy and apoptosis (Hannun and Obeid, 2008; Kitatani et al., 2008; Lahiri and Futerman, 2007).

Sphingolipids consist of a sphingoid base linked to a variety of polar groups and fatty acid chains (Hannun and Obeid, 2008). SPL metabolism is well regulated and compartmentalized, and ceramide (CER), the core member of the family, can be generated from multiple metabolic pathways in response to different stimuli: 1) the *de novo* pathway (stress and apoptosis) starting from the condensation of serine and fatty acyl-CoA; 2) the sphingomyelinase (SMase) pathway, whereby CER is obtained after the hydrolysis of the sphingomyelin (SM) by the SMases (oxidative stress and treatments with TNF-α); 3) the salvage pathway, which consists of the break down of complex sphingolipids to sphingosine (SPH), which can produce CER after reacylation, and is related to growth arrest, cellular signaling and trafficking; and 4) the recycling pathway where exogenous short-chain CERs are deacylated and reacylated (Kitatani et al., 2008).

To date, several syndromic diseases are caused by dysfunction of SPL metabolism. These sphingolipidoses are lysosomal hereditary disorders due to mutations in the genes encoding enzymes involved in SPL metabolism. Examples include Gaucher (β-glucocerebrosidase), Niemann-Pick A/B (acid sphingomyelinase), and Farber (acid ceramidase) syndromes (Fox et al., 2006). In several cases, the patients show loss of vision caused by retinal cell degeneration as a secondary trait (Brush et al., 2010). Mutations in other lipid-related genes cause severe retinal dystrophies: ELOVL4, an elongase of very long chain fatty acids (Agbaga et al., 2008), causes autosomal dominant Stargardt disease type 3, STGD3; the transporter ABCA4 causes autosomal recessive Stargardt disease type 1, STGD1; and mutation in the acyltransferase LRAT, which catalyzes the esterification of all-trans-retinol, causes autosomal recessive retinitis pigmentosa and Leber congenital amaurosis (RP and LCA, respectively) (Ruiz et al., 1999). Although little is known about the precise role of SPLs in the retina, CER levels have been shown to increase during retinal degeneration (Chen et al., 2012; German et al., 2006; Sanvicens and Cotter, 2006). Moreover, in RP models the structure and function of photoreceptor cells is preserved when CER synthesis is inhibited (Strettoi et al., 2010). SPH is also considered a pro-apoptotic molecule (Abrahan et al., 2010), whereas the phosphorylated forms of SPH and CER (S1P and C1P, respectively)

play opposite roles and promote retinal cell survival and division (Miranda et al., 2011, 2009). Overall, SPL metabolism serves as a rheostat that controls cell fate and operates under tight regulation.

CERKL (*CER Kinase-Like*) is an autosomal recessive RP and cone–rod dystrophy (CRD) causative gene that shares high homology (29% identities and 50% similarity) with the human CERK (Tuson et al., 2004). To date, 7 mutations have been associated with retinal dystrophies; the R257X nonsense variant was the first described and the most prevalent mutation in the Spanish population (Aleman et al., 2009; Ali et al., 2008; Auslender et al., 2007; Avila-Fernandez et al., 2010, 2008; Littink et al., 2010; Pomares et al., 2007; Tang et al., 2009; Tuson et al., 2004). CERKL contains 2 nuclear localization (Inagaki et al., 2006) and 2 export signals (Rovina et al., 2009), a pleckstrin homology region (PH) (Rovina et al., 2009), and a conserved lipid kinase domain (DAGK) (Bornancin et al., 2005; Tuson et al., 2004). It also shows a dynamic subcellular localization, mainly associated to membranes (Tuson et al., 2009), and the retinal expression of the gene in mouse revealed high expression in the ganglion cell layer and moderate expression in photoreceptors and the inner nuclear layer (Garanto et al., 2012; Tuson et al., 2004). At the protein level, CERKL co-localizes with ganglion, amacrine, bipolar and cone cell markers (Garanto et al., 2011, 2012; Vekslin and Ben-Yosef, 2011).

The presence of a conserved DAGK domain and the high homology with CERK has supported a CER kinase role for CERKL. However, after many attempts by several groups, CERKL remains a lipid orphan kinase, as its substrate is still unknown and its kinase activity under debate (Bornancin et al., 2005; Inagaki et al., 2006; Nevet et al., 2012; Tuson et al., 2009). Two mouse models have been generated. The first, created by deletion of the alternatively spliced exon 5, where the most prevalent mutation (R257X) is found, affects only some *CERKL* isoforms, and does not show any phenotype (Graf et al., 2008). The second mouse model (referred in the text as *Cerkl* −/− or KO) was generated in our group by deletion of the proximal promoter and exon 1. The targeted *Cerkl* deletion resulted in a knockdown rather than a full knockout model due to transcription from two previously unreported alternative promoters (Garanto et al., 2012). Both models were viable and fertile, and did not show any gross morphological alterations in their retinas. However, the detailed analysis of the *Cerkl* −/− model revealed an increase in retinal apoptosis and gliosis, alterations in the oscillatory potentials of the electroretinographic recordings, and a decrease of the ganglion cell marker Brn3a, suggesting a dysfunction of the ganglion and/or amacrine rather than photoreceptor cells (Garanto et al., 2012).

After exhaustive SPL quantification by UPLC-TOF, the sphingolipid, phospholipid and neutral lipid profiles of wild-type mouse retinas is here presented, and then compared to that of the *Cerkl* −/− model. Also, several lipids have been assayed *in vitro* as potential CERKL substrates. Our results describe for the first time the SPL content of the wild type mouse retina and report significant and specific decreases (mainly ranging from 30% to 60%) in the SPL content in the retinas of *Cerkl* −/− mice, whereas the phospholipids and neutral lipids remain unaltered. Overall, our data indicate the involvement of CERKL in SPL metabolism, but do not support its role as a lipid kinase.

2. Material and methods

2.1. Animal handling and tissue dissection

Murine tissue samples were obtained from six *Cerkl* +/+ and *Cerkl* −/− C57BL/6J background mice. All procedures were performed according to ARVO statement for the use of animals in ophthalmic and vision research, and all the protocols were approved by the Animal Care facilities at the University of Barcelona Guidelines for Animals in Research and the Institutional Animal Care and Use Committees of the University of Oklahoma Health Sciences Center and the Dean McGee Eye Institute. Animals were euthanized with CO2 followed by cervical dislocation. Whole retinas were dissected and immediately frozen in liquid nitrogen.

2.2. Sample preparation

Each pair of retinas from the *Cerkl* +/+ (n = 6) and *Cerkl* −/− (n = 6) mice were homogenized by Polytron PT 1200 E homogenizer (Kinematica AG, Lucerne, Switzerland) (15 s on ice) in 300 μl of buffer containing 25 mM KCl, 50 mM Tris-HCl (pH 7.5), 0.5 mM EDTA and 0.25 M sucrose. Protein quantification was carried out by BCA kit (Thermo Fisher Scientific, Rockford, IL) and was used to normalize lipidomic results.

2.3. Lipid extraction

Lipid extraction was performed by a modification of the Folch's method (Folch et al., 1957). Briefly, 25 μl of the homogenized retinas were mixed with 1 ml of chloroform (C) and 0.25 ml of methanol (M). Internal standards were also added at this point (200 pmol of C17/C17-PC, C17/C17-PE and C17/C17-PS). Samples were heated at 48 °C overnight and next day samples were dried under N2.

Sphingolipid extraction was performed following the protocol described by Merrill et al. (2005) with some modifications. Briefly, 125 μl of the homogenized retinas were mixed with 0.5 ml of M and 0.25 μl of C. Internal standards were also added at this point (200 pmol of C12 species of CER, SM, and GlcCer). Samples were heated at 48 °C overnight. Next day, 75 μl of 1 M KOH in methanol were added, followed by a 2-h incubation at 37 °C. Finally, the mixtures were neutralized with 75 μl of 1 M acetic acid, and dried under N2.

2.4. Lipidomics

Lipid extracts were solubilized in 150 μl of methanol. The liquid chromatography-mass spectrometer consisted of a Waters Aquity UPLC system connected to a Waters LCT Premier Orthogonal Accelerated Time of Flight Mass Spectrometer (Waters, Millford, MA), operated in positive or negative electrospray ionization mode. Full scan spectra from 50 to 1500 Da were obtained. Mass accuracy and reproducibility were maintained by using an independent reference spray via LockSpray. A 100 mm × 2.1 mm id, 1.7 μm C8 Acquity UPLC BEH (Waters) analytical column was used. The two mobile phases were 1 mM ammonium formate in methanol (phase A) and 2 mM ammonium formate in H2O (phase B), both phases with 0.05 mM of formic acid. Two gradients were programmed: gradient I: 0 min, 80% A; 3 min, 90% A; 6 min, 90% A; 15 min, 99% A; 18 min, 99% A; 20 min, 80% A and gradient II: 0 min, 65% A; 2 min, 65% A; 5 min, 90% A; 11 min, 99% A; 12 min, 99%

A; 14 min, 65% A. In both cases, the flow rate was 0.3 ml min^{-1}. The column was run at 30 °C. Quantification was carried out using the ion chromatogram obtained for each compound using 50 mDa windows. The linear dynamic range was determined by injection of standard mixtures. Positive identification of compounds was based on the accurate mass measurement with an error <5 ppm and its LC retention time, compared to that of a standard (±2%).

Annotation of lipid species: Glycerophospholipids, diacylglycerol, triacylglycerol and cholesterylesters were annotated as <lipid subclass> <total fatty acyl chain length>:<total number of unsaturated bonds>. Plasmalogen were annotated as above except that <p> was added at the end. Sphingolipids were annotated as <lipid subclass> <total fatty acyl chain length>:<total number of unsaturated bonds>. If the sphingoid base residue was dihydrosphingosine the lipid class contained a <DH> prefix.

Data analysis and presentation: Lipid levels for each sample were calculated when the corresponding internal standard was available in our laboratory. In the absence of IS, values were estimated relative to an added reference and indicated as equivalents. LacCer, GM3 and sulfatides were referred to GlcCer C12; DAG, TAG and CE were referred to C17:0/C17:0-PC and PI were referred to C17:0/C17:0-PE. The final data are presented as mean ± SD.

2.5. RNA extraction and RT-PCR

Twenty-five mg of each frozen mouse tissue were homogenized using a Polytron PT 1200 E homogenizer (Kinematica AG, Lucerne, Switzerland). For total RNA extraction, High Pure RNA Tissue Kit (Roche Diagnostics, Indianapolis, IN) was used, following the manufacturer's instructions. Total RNA was quantified using the Nanoquant plate in an Infinite 200 microplate reader (Tecan, Männedorf, Switzerland). The RT-PCR assay was carried out with the Transcriptor High Fidelity cDNA Synthesis Kit (Roche Diagnostics, Indianapolis, IN) performed following the manufacturer's protocol, using 200 ng of mouse total RNA. For expression analysis, all reactions (50 µl) contained 10 µM of each primer pair, 2 µM of dNTPs, 1.5 mM $MgCl_2$ and 1 U of Go*Taq* polymerase (Promega, Madison, WI). Mouse *Gapdh* expression was used to compare and normalize the samples. PCR conditions for all the analyzed genes were as follows: 120 s at 94 °C and 30–35 cycles of 94 °C for 20 s and 55/58/60 °C (depending on the oligonucleotide pair) for 30 s and 72 °C for 30 s. Oligonucleotide sequences are listed in Table 1.

2.6. Cell culture and transfection

HEK293T cells (Human Embryonic Kidney Cells 293T) were grown in DMEM with 4 mM L-glutamine, supplemented with 10% fetal bovine serum (FBS), 100 U/ml of penicillin and 100 µg/ml streptomycin (Invitrogen Life Technologies, Carlsbad, CA). Cells were transfected with pcDNA3 empty (Invitrogen Life Technologies, Carlsbad, CA) or containing the CERKL isoforms fused to the HA epitope at the C-terminus of the protein (Tuson et al., 2009). All transient transfections were performed using Lipofectamine TM 2000 (Invitrogen Life Technologies, Carlsbad, CA) according to the manufacturer's protocol. Cells were harvested 48 h after transfection, rinsed in PBS and lysed by sonication in 20 mM MOPS

(pH 7.2), 2 mM EGTA, 10% glycerol, and 1 mM DTT. Protein quantification was performed with the BCA kit (Thermo Fisher Scientific, Rockford, IL). Transfection efficiencies were assessed by Western-Blot.

2.7. Protein–lipid overlay

Protein–lipid overlay was carried out following reported protocols (Dowler et al., 2002). Briefly, 50–100 μg of commercial lipids (Matreya LLC, Pleasant Gap, PA and Sigma–Aldrich, Saint Louis, MO) were dried under N2 and resuspended in 5 μl of C:M:H_2O (1:2:0.8). Afterward, lipids were spotted on a Hybond C-extra membrane (GE Healthcare, Waukesha, WI) and dried for 1 h at RT. Membranes were incubated in blocking solution [1% BSA, 1% non-fatty milk in TBS-50 mM Tris-HCl (pH 7.5) and 150 mM NaCl] for 1 h, followed by an overnight incubation at 4 °C in 1 μg/μl – protein lysates in blocking solution. Next morning, membranes were rinsed 10 times in TBST (TBS and 0.1% Tween) for 5 min. Immunodetection was performed with a primary monoclonal antibody anti-HA (1:1000) for 2 h, then rinsed 10 times for 5 min in TBST; incubated for 1 h with HRP-conjugated anti-mouse secondary antibody (1:3000) and washed 12 times in TBST. Finally, membrane was developed with the ECL detection system (Thermo Fisher Scientific, Rockford, IL).

For bovine retinal lipid extraction, 200 mg of tissue were homogenized in 500 μl of 1 mM DTPA and transferred to a new tube (it was repeated twice), 1 ml of 1 mM DTPA and 4 ml of C:M (1:1) were added to each tube. Tubes were capped under N_2, mixed, and sonicated for 30 min. Then, the lower layer was first recovered after a centrifugation step at 7000 rpm for 10 min. Two additional ml of C were added to the remaining upper layer for a second extraction. The two recovered layers were combined and 1 ml of C:M:1 mM DTPA (3:48:47) was added and centrifuged for 10 min at 7000 rpm. The upper layer was discarded and the remaining lower phase was dried down under N_2.

2.8. Enzymatic reaction and phosphorus assay

Reactions were performed as described previously (Tuson et al., 2009). Micelles containing a mixture of commercial lipids grouped according to their chemical properties (a total of 100 μg of lipids per group) were mixed with lysates of cells transfected with pcDNA (empty vector) or pcDNA-CERKLa (Fig. 8C). The phosphorus assay was started by adding 0.26 ml of 70% perchloric acid, incubating for 1 h at 185 °C and chilling on ice for 5 min. After the incubation, 0.92 ml of H_2O were added and the reactions were mixed with 0.4 ml of 1.25% ammonium molybdate and 0.4 ml of 5% ascorbic acid. Samples were incubated at 100 °C for 5 min, chilled on ice for another 5 min and the absorbance was measured at 797 nm. The amount of phosphorus was calculated by performing a standard curve at different amounts of Na_2HPO_4 at 0.1 μg/μl of phosphorus. At least 3 replicates were analyzed per group of lipids. Phosphorus of micelles as well as of cell lysates was also quantified.

3. Results

3.1. Lipidomics of wild-type and Cerkl −/− retinas

Ceramide is a core molecule of the SPL metabolism and is generated *de novo* by condensation of serine and palmitoyl-CoA. CER is the precursor of the SPH and C1P, as

well as other complex sphingolipids, such as SM and glycoSPLs (Fig. 1). High levels of CER trigger apoptosis, thus cells need to rapidly convert CER to other SPLs to escape this fate. The characterization of the retinal SPL content in WT and *Cerkl* −/− (KO) was performed by UPLC-TOF on retinas of 6 different P60 animals of each genotype. The statistical analysis relied on the Mann–Whitney test. For the sake of clarity, the data are visualized as histograms. The total numerical values and quantification of each species are shown in the Supplementary Tables 1 and 2, respectively.

3.1.1. Retinal sphingolipid content in wild type and Cerkl −/− mice—UPLC-TOF analyses showed different peaks for each SPL species–defined by the carbon length of the fatty acid chain linked to the sphingoid base-, which were quantified by using a standard lipid mix (see the details in the Material and methods). The sum of all the saturated and unsaturated SPL species is represented in Fig. 2. SM is the main SPL in the mouse retina reaching up to 8 nmol/mg of total protein (referred from now onwards as nmol/mg), and accounting for the 80% of all the SPLs analyzed. CERs are the second more abundant group (around 11% of the total) with levels of 1 nmol/mg. The next group is the glycoSPLs, where the sum of GalCer and GlcCer –both share the same mass and are not resolvable by the UPLC used conditions, and will be referred from now onwards as monohexosylceramides (MHCer)– accounts for almost 4% of the total. GlcCer is the precursor of LacCer, which produces GM3 and other gangliosides, whereas GalCer generates the sulfatide species. DhCer (0.14%) is the preceding metabolite of CER in the *de novo* pathway, and of the DhSM(1.6%of the total SPLs) after addition of a phosphocholine group. The CER derivative sphingosine (SPH) accounts for 0.45% of the total SPLs.

Once the WT mouse retinas were characterized, we aimed to analyze the SPLs content in the *Cerkl* −/− retinas in order to assess the possible effect of *Cerkl* depletion on SPL metabolism. Notably, statistically significant differences were observed for almost all SPLs. The highest decrease (58%) was found in the MHCer group. DhCER, GM3 and SPH all decrease around 41%. SM, DhSM and CER also showed a significant decrease (40–31%). LacCER and sulfatide groups are also decreased but the differences were not significant.

These results prompted us to investigate in detail the species composition of each SPL. Using this methodology, SPLs from 14 up to 28 carbon chains were detected and quantified.

3.1.2. Ceramides—The retinal CER species content of WT retinas is depicted in Fig. 3A. This analysis revealed that saturated C16 and C18 are the most abundant CERs (at equivalent levels) in the retina, followed by the C20, C22 and C24 species, the less frequent saturated CERs being C14, C26 and C28 (below 3 pmol/mg). Regarding the unsaturated CERs the most abundant species are C18:1 and C24:1 (around 91–61 pmol/mg respectively) followed by C16:1, C20:1, C24:2 and C22:1 (between 40 and 26 pmol/mg). Notably, KO samples showed consistent decreased levels of all CER species, particularly for saturated C24:0, and C28:0 CERs (decreases of 47% and 62%), and unsaturated species C18:1, C20:1, C22:1 and C24:1 and C24:2 (decreases of 40–50% in all the cases).

3.1.3. Sphingomyelins—SM is a complex SPL with a phosphocholine as its polar group. It is the most representative SPL group in the retina (Fig. 2) (Brush et al., 2010). After

detailed quantification of the SM species in the WT retinas (Fig. 3B), C16–C18 were clearly the most abundant (reaching levels around 2.5 nmol/mg). In contrast, short and long chain SMs were detected at low levels. When comparing *Cerkl* −/− to WT (Fig. 3B), a significant decrease was observed in the same carbon length chain species as detected for CERs (C16:0, C18:0, C20:0, C22:0, C24:0, C16:1, C18:1, C20:1, C22:1 and C24:2), which is consistent with CER being the immediate precursor of SM.

3.1.4. Dihydroceramides and dihydrosphingomyelins—Recent evidence has shown that DhSPLs, otherwise considered inactive precursors of CERs, are biologically active SPLs (reviewed in Fabrias et al. (2012)) and as such, they have also been identified and quantified. In mouse WT retinas, the C16 and C18-DhSPL species were shown to be the most abundant (Fig. 3C and D). When comparing KO vs WT retinas, statistically significant decreases were detected for all the C chain length DhCER, ranging from 30% to 65% (Fig. 3C). These decreases were also observed in the DhSM derivatives, but were only significant for the C16 and C22 species (Fig. 3D).

3.1.5. Glycosphingolipids—Glycosphingolipids are a group of complex SPLs derived from CER, where carbohydrate moieties are added as polar groups. The simplest molecules are GlcCer and GalCer (referred as MHCer), which contain a glucose and a galactose, respectively (Fig. 1). LacCer, GM3 and other gangliosides are generated from GlcCer, whereas sulfatides are derived from GalCer, upon successive addition of saccharide molecules.

In the WT retinas MHCer from 16 to 26 carbon atoms were detected by UPLC-TOF. Of those, the most abundant species was C22, followed by C20 and C24 (Fig. 4A). Undetectable or very low amounts of C14 and C26 species were also observed in this group, but they were not observed in the downstream LacCer, GM3, and sulfatide groups. With respect to the unsaturated GlycoSPLs, only the C24:1 species, either in the MHCer or the GlcCer-derived molecules, were detected.

Regarding LacCers in WT retinas, all species showed similar levels except for C16 and C18, whose amount doubled those of the rest (Fig. 4B). In contrast, the most abundant species of its immediate derivative, GM3, was C16 (Fig. 4C). For GalCer-derived products, only two C16 sulfatides, SGPCaOH and SGdHC, could be detected (Fig. 4D).

When comparing *Cerkl* −/− to WT retinas, and as it happened with CERs and SMs, almost all MHCer species were significantly diminished, showing a dramatic reduction of 45–85% in all species (Fig. 4A). When considering LacCers, the same reduction trend was observed (Fig. 4B). With respect to GM3 and sulfatides (Fig. 4C and D), the downward tendency was maintained for both, being statistically significant for C18 and C20 GM3 species.

3.1.6. Sphingosine—One of the key contributors to the sphingolipid signaling is sphingosine and its derivatives. The amount of sphingosines is much lower than that of ceramides in WT retinas. Notably, *Cerkl* −/− retinas show a statistically significant decrease (42%) in sphingosine levels (Fig. 2 and Supplementary Tables 1 and 2). The

dihydrosphingosine contribution to the mouse retina lipid pool (in both WT and KO retinas) was below the detection level and has been quoted as not detectable (ND).

3.1.7. Phospholipid and neutral lipid content—In order to explore whether the changes in SPL content in KO retinas were a general trend of many lipid species or were specific to the SPL group, we quantified other relevant retinal lipids, such as phospholipids (PL) and neutral lipids (NL) to compare the contents in WT and KO retinas. The total fatty acid pool was not amenable to our analysis due to the extraction procedure, designed for optimal sphingolipid yield.

The main PL (phosphatidylcholine, phosphatidylethanolamine, phosphatidylinositol, phosphatidylserine and plasmalogen) and NL (diacylglycerol, triacylglycerol and cholesterol ester) groups were quantified and compared between WT and KO retinas (Fig. 5).

The comparison of WT and *Cerkl* −/− samples did not show any differences either in the analyzed PL or NL content. These results strongly support that the decrease in the SPL levels is specific and restricted to the SPL group of lipids, and it cannot be considered a general trend.

3.2. Trancriptional analysis of SPL genes

CERKL protein is mainly associated with cytoplasmic membranes, but shows a dynamic subcellular localization, shifting from cytosol to nucleus (Tuson et al., 2009) where it could, directly or indirectly, regulate gene transcription. In order to assess whether the observed decrease in SPL metabolites in *Cerkl* −/− retinas was due to gene downregulation caused by CERKL depletion, the expression of putative target genes was analyzed. As the differences in the sphingolipidome were mainly detected in SM, Glc/GalCer and CER, the transcriptional levels of the genes involved in their synthesis (CER: *Degs1* and *Degs2*, GlcCer: *Uggt1* and *Uggt2*, GalCer: *Ugt8a*: SM: *Sgms1* and *Sgms2*) were compared in WT vs KO mouse retinas. Known SPL kinases (*Cerk*, *Sphk1* and *Sphk2*), as well as reported CER and GlcCER transporters (*Cert* and *Fapp2*), were also included. *Gapdh* and *Cerkl* expression were used for normalization and control, respectively (Fig. 6).

As reported, semiquantitative analysis showed reduced *Cerkl* expression levels (around 70%) in the *Cerkl* −/− retinas (Garanto et al., 2012). In contrast, no significant differences were detected in the transcription levels of the assessed genes (Fig. 6), ruling out any CERKL effect on the expression of these genes.

Among the analyzed genes, we were unable to detect expression of *Ugt8a* and *Sgms2* either in WT or KO retinas. This could be due to very low, if any, transcription levels because of gene redundancy, or that they produce unreported transcripts in the retina, not detectable in our conditions.

3.3. Enzymatic activity and phosphorus incorporation

Since CERKL was described in 2004 by our group, several groups have attempted, unsuccessfully so far, to show its kinase activity (Bornancin et al., 2005; Inagaki et al., 2006; Nevet et al., 2012; Tuson et al., 2009). We aimed to identify this activity among

tissue-specific substrates and complement previous attempts that had only assessed the standard CERs (C16–C20). CERs with very long chain fatty acids (VLCFA) were recently identified in rodent retinas, testes and skin (Brush et al., 2010), but were infrequent in other tissues. Based on previous data showing that overexpression of ELOVL4 in cultured cells resulted in the biosynthesis of VLCFA that could be later incorporated to sphingolipids (Agbaga et al., 2008), we aimed to test whether CERKL phosphorylated the VLCCERs under these conditions. No evidence in favor of a kinase function for CERKL upon standard or VLCCERs could be gathered (Suppl. Fig. 1).

These negative results prompted us to test the kinase activity of CERKL upon micelles containing a combination of either SPL or non-SPL compounds, by colorimetric quantification of phosphorus incorporation. To evaluate the sensitivity of the assay, protein lysates from CERK-overexpressing cells added to micelles containing a mixture of ceramides were used as a positive control. Our results showed a statistically significant increase on the amount of phosphorus incorporated in CERK-overexpressing cells, whereas lysates of cells transfected with CERKL and pcDNA empty vector did not show any difference (Fig. 7A). As a second step micelles were generated by combining groups of lipids according to their chemical properties (Fig. 7B). The negative controls were reactions with protein lysates with empty micelles (group 0), and micelles without protein lysates (first bar of each group). No significant differences were observed between lysates of HEK293T cells transfected with empty pcDNA compared to those overexpressing CERKL (Fig. 7C). In addition, no hints of an unidentified endogenous phosphorylated substrate (lipid or protein) in CERKL-overexpressing lysates could be observed when empty micelles were added (Fig. 7C), arguing against any type of kinase activity associated to CERKL.

3.4. CERKL binds to some complex sphingolipids

Cerkl −/− sphingolipidome showed significant decreases in SM, CER and Glc/GalCer levels compared to WT retinas. These results prompted us to explore by protein–lipid overlay whether CERKL could interact with lipids.

A collection of isolated commercial lipids and SPLs were spotted and immobilized onto nitrocellulose membranes before incubation with protein lysates. Total bovine retinal lipids (RL) were also added as a positive control. Protein lysates were obtained from HEK293T transfected with, either pcDNA empty vector, the most common CERKL isoform (CERKLa), or a mixture of four CERKL retina isoforms produced by alternative splicing (CERKLa, CERKLb, CERKLc and CERKLd). Our results showed that CERKL consistently recognized SM, GlcCer (Fig. 8A) and GalCer (Fig. 8B). However, CERKL binding was not detected with CER, LacCer, GM1 or any FFA (Fig. 8B). Cisretinol and retinoic acid (RA) were also tested (Fig. 8A). Although some signal was detected for RA, it was discarded as it was also detected in the negative control (pcDNA lysates, Fig. 8A).

4. Discussion

4.1. Sphingolipidome of the retina

To our knowledge, no comprehensive analysis of the SPL content of the human and mouse retina has been reported, despite the increasing relevance of SPLs in regulating key

developmental and cell processes. On the one hand, SPL metabolism dysfunction has been involved in severe syndromic pathologies with retinal degeneration. On the other hand, our group identified *CERKL* as a retinal dystrophy causative gene, and the encoded protein shared considerable overall homology with the ceramide kinase protein (CERK) that set the grounds for a new link between SPLs and retinal function. Therefore, our first aim was to provide a retinal SPL profile useful for both, those focused on SPL research, and to approach CERKL function and characterize its substrate. We set out to compare the WT retinal sphingolipidome with that of our recently generated *Cerkl* −/− model.

This work presents extensive SPL quantification data (absolute and relative values listed in Supplementary Tables 1 and 2), but we will focus on the most relevant components in the retina and highlight the differences identified between the WT and KO model. Concerning the first aim, SM stands out as the most abundant SPL in the retina, in agreement with reports of other neuronal tissues, stressing its contribution to the structure of the myelin sheath, clustering of lipid rafts, and fluidity of cell membranes (Brush et al., 2010; Mencarelli and Martinez-Martinez, 2012). Concerning the length of the carbon atom chains, C16 and C18 species are the most common for CER, SM, LacCer, GM3, DhCER and DhSM groups, whereas the C20 and C22 are the most frequent MHCer. Although no comparable comprehensive study has been described, our results (when calculated as percentages of major sphingolipids) are in agreement with previous semiquantitative data on rat retina (Fox et al., 2006; Brush et al., 2010), a partial study on the mouse retina (Graf et al., 2008), and mammal brain (Mencarelli and Martinez-Martinez, 2012) CERs.

Our quantification of other retinal lipids (PLs and NLs) is in accordance with previous lipidomic analysis in rat (Ford et al., 2008), human (Acar et al., 2012) and bovine retinas (Brush et al., 2010).

Overall, our results are in agreement with previous partial reports but expand the picture by providing a full overview of the SPL content in the retina, which could be an invaluable reference for the study of the SPL metabolism in health and disease.

4.2. Cerkl −/− retinas show decreased levels of sphingolipids

Once the retinal SPL content in WT mice was established, we aimed to characterize the sphingolipidome of the *Cerkl* −/− retinas and compare it to the WT. Interestingly, a general decrease in the SPL content of *Cerkl* −/− was observed, being MHCer the group with the greatest reduction (close to 60%), followed by GM3, SPH and DhCER (41%), SMs (38%) and CERs (close to 30%). Of note, the highest decreases in SPL content between KO and WT retinas clustered around CER and its close metabolites, particularly evident for the MHCer group (Fig.2 and Supplementary Tables 1 and 2). Contrary, concerning the PL and NL content no differences were observed, indeed supporting that the alterations detected in the KO lipid quantification solely affected the SPL family.

Overall, these results highlight the role, as yet unassigned, of CERKL in SPL metabolism, particularly in relation to CER and/or its immediate derivatives. Considering that this *Cerkl* model is a knockdown that retains as much as 35% of *Cerkl* transcription, it is tempting to

speculate that a complete null genotype would show a further decrease in SPLs, associated with a more severe retinal disorder.

4.3. CERKL is most probably not a kinase

During the past years the repeated attempts of several groups to assign a CER kinase function for CERKL based on its homology to CERK have proved fruitless. CERKL does not phosphorylate standard CERs under the reaction conditions of CERK (Bornancin et al., 2005; Inagaki et al., 2006; Tuson et al., 2009), Ca^{2+} depletion (Nevet et al., 2012), different pHs (Garanto, 2011), or in the presence of GTP instead of ATP (Garanto, 2011). To approach the identification of the putative substrate from a different angle, we tried two new strategies testing: i) very long chain fatty acid CERs as CERKL substrates, based on the recent results describing the function of the ELOVL4 protein (involved in the STGD3 retinal dystrophy) as a FA elongase of VLCFA(C28–C30) and VLCPUFA (C28–C38) (Agbaga et al., 2008); and ii) phosphorus incorporation in micelle-protein lysate combined assays. Indeed, CERKL did not phosphorylate VLCCERs, neither promoted any phosphorus incorporation in CERKL lysates upon a set of lipid-combined micelles. A test for ATPase activity (phosphatase instead of kinase) of CERKL was also negative (Garanto, 2011). Overall, our data together with other reports by different groups, clearly argue against CERKL being a lipid kinase and point to functional roles other than lipid phosphorylation.

4.4. CERKL is not involved in the transcriptional regulation of SPL genes

The dynamic subcellular localization of CERKL suggested different roles in the nucleus and cytoplasm (Tuson et al., 2009). Based on our lipidomic analyses showing a general decrease in SPLs, especially in complex SPLs, we hypothesized CERKL contribution to transcription regulation of the genes involved in the SPL metabolism. However, the analysis in our model showed that *Cerkl* depletion did not affect the expression of SPL-related genes in the retina. Therefore, the decrease of several SPLs is not caused by dysregulation of the SPL synthesis genes, supporting that CERKL is related to SPL metabolism, but neither as a transcription factor nor as a kinase.

4.5. CERKL binds to complex SPLs

We also assessed the capacity of CERKL to bind to SPLs in protein–lipid overlay assays. The positive control, CERK, was consistently able to bind to CERs (Garanto, 2011), whereas CERKL was not. Among the several lipids analyzed (including a wide range of SPLs), positive CERKL binding was obtained for GlcCer, SM and GalCer, in full agreement with the SPL groups in the *Cerkl* −/− retinas showing the highest reduction at maximum statistical significance.

4.6. What next? CERKL function and future directions

CERKL was the first candidate to directly link retinal dystrophies and SPLs, and this assumption was based on *in silico* protein homology with CERK. Nowadays, it seems to be clear that CERKL does not have kinase activity, unless it acts on very rare lipids. A protein is usually defined by what it does rather than what it does not, but so far CERKL illustrates

the hard way to uncover the function of proteins not acting in their predicted roles, and when advances in knowledge first means exploring possibilities and discarding them one by one.

SPLs play essential roles triggering apoptosis or promoting cell survival: high levels of CER induces apoptosis, whereas C1P promotes cell proliferation and GlcCer acts as anti-apoptotic agent in oxidative stress conditions (Hirabayashi, 2012; Rotstein et al., 2010). Overexpression of CERKL protects cultured cells from oxidative stress injury (Tuson et al., 2009). On the other hand, CERKL binds to GlcCer, and depletion of CERKL causes a relevant decrease of Glc/GalCers. These results may indicate that CERKL and GlcCer work together against oxidative stress. Indeed, new experiments are required to elucidate the function of CERKL–GlcCer interaction.

In conclusion, we provide an exhaustive sphingolipidome for the WT mouse retina and compare it to that of the *Cerkl* −/− model. The depletion of *Cerkl* in the KO model caused a relevant and consistent decrease in retina SPL content, mainly for MHCers, SMs and CERs, but did not alter the transcriptional levels of SPL-related genes. Although it contains a lipid kinase domain and shares high homology with CERK, CERKL did not show any kinase activity on standard CERs, VLCCERs, and other SPLs, FFAs, or phospholipids. Moreover, we show binding of CERKL to GlcCer, SM, GalCer, and total bovine retinal lipids. All together, these results support a relevant involvement of CERKL in SPL metabolism, but not as a kinase. Further work will be required to investigate CERKL interaction with GlcCer and other SPLs, and its contribution to SPL metabolism and other key cell functions, such as protection against oxidative stress, and eventually, unveil the pathway linking CERKL mutations to retinal dystrophies.

Supplementary Material

Refer to Web version on PubMed Central for supplementary material.

Acknowledgments

We would like to thank Eva Dalmau, Julie-Thu Tran and Victor Abad for technical support. Martin- Paul Agbaga, Michael Elliott and Steve Brush for their suggestions and ideas to improve the manuscript. A.G was in receipt of the fellowship FPI BES-2007-15414 and the short stay fellowships “Ayudas a la movilidad CIBERER 2008” and “Programa de estancias breves FPI 2009” to visit Dean McGee Eye Institute in Oklahoma City (USA).

Grant information: This study was supported by grants BFU2006-04562 (Ministerio de Educación y Ciencia), SAF2009-08079 (Ministerio de Ciencia e Innovación), 2009SGR-1427 (Generalitat de Catalunya), CIBERER (U718), Retina Asturias and ONCE to R.G.-D; BFU2010-15656 (Ministerio de Educación y Ciencia) to G. M. SAF 2011-22444 (Ministry of Science and Innovation) and 2009SGR1072 (Agència de Gestió d'Ajuts Universitaris i de Recerca de la Generalitat de Catalunya) to G.F. and project 112130 from Fundació Marató de TV3 to JC. This work was also supported by NIH Grants EY00871, EY04149, EY12190, EY21725, EY 022071 and RR17703; Foundation Fighting Blindness and Research to Prevent Blindness to R.E.A and N.A.M.

References

Abrahan CE, Miranda GE, Agnolazza DL, Politi LE, Rotstein NP. Synthesis of sphingosine is essential for oxidative stress-induced apoptosis of photoreceptors. Invest Ophthalmol Vis Sci. 2010; 51:1171–1180. [PubMed: 19797232]

Acar N, Berdeaux O, Gregoire S, Cabaret S, Martine L, Gain P, Thuret G, Creuzot-Garcher CP, Bron AM, Bretillon L. Lipid composition of the human eye: are red blood cells a good mirror of retinal and optic nerve fatty acids? PLoS One. 2012; 7:e35102. [PubMed: 22496896]

Agbaga MP, Brush RS, Mandal MN, Henry K, Elliott MH, Anderson RE. Role of Stargardt-3 macular dystrophy protein (ELOVL4) in the biosynthesis of very long chain fatty acids. Proc Natl Acad Sci U S A. 2008; 105:12843–12848. [PubMed: 18728184]

Aleman TS, Soumittra N, Cideciyan AV, Sumaroka AM, Ramprasad VL, Herrera W, Windsor EA, Schwartz SB, Russell RC, Roman AJ, Inglehearn CF, Kumaramanickavel G, Stone EM, Fishman GA, Jacobson SG. CERKL mutations cause an autosomal recessive cone-rod dystrophy with inner retinopathy. Invest Ophthalmol Vis Sci. 2009; 50:5944–5954. [PubMed: 19578027]

Ali M, Ramprasad VL, Soumittra N, Mohamed MD, Jafri H, Rashid Y, Danciger M, McKibbin M, Kumaramanickavel G, Inglehearn CF. A missense mutation in the nuclear localization signal sequence of CERKL (p.R106S) causes autosomal recessive retinal degeneration. Mol Vis. 2008; 14:1960–1964. [PubMed: 18978954]

Auslender N, Sharon D, Abbasi AH, Garzozi HJ, Banin E, Ben-Yosef T. A common founder mutation of CERKL underlies autosomal recessive retinal degeneration with early macular involvement among Yemenite Jews. Invest Ophthalmol Vis Sci. 2007; 48:5431–5438. [PubMed: 18055789]

Avila-Fernandez A, Cantalapiedra D, Aller E, Vallespin E, Aguirre-Lamban J, Blanco-Kelly F, Corton M, Riveiro-Alvarez R, Allikmets R, Trujillo-Tiebas MJ, Millan JM, Cremers FP, Ayuso C. Mutation analysis of 272 Spanish families affected by autosomal recessive retinitis pigmentosa using a genotyping microarray. Mol Vis. 2010; 16:2550–2558. [PubMed: 21151602]

Avila-Fernandez A, Riveiro-Alvarez R, Vallespin E, Wilke R, Tapias I, Cantalapiedra D, Aguirre-Lamban J, Gimenez A, Trujillo-Tiebas MJ, Ayuso C. CERKL mutations and associated phenotypes in seven Spanish families with autosomal recessive retinitis pigmentosa. Invest Ophthalmol Vis Sci. 2008; 49:2709–2713. [PubMed: 18515597]

Bornancin F, Mechtcheriakova D, Stora S, Graf C, Wlachos A, Devay P, Urtz N, Baumruker T, Billich A. Characterization of a ceramide kinase-like protein. Biochim Biophys Acta. 2005; 1687:31–43. [PubMed: 15708351]

Brush RS, Tran JT, Henry KR, McClellan ME, Elliott MH, Mandal MN. Retinal sphingolipids and their very-long-chain fatty acid-containing species. Invest Ophthalmol Vis Sci. 2010; 51:4422–4431. [PubMed: 20393115]

Chen H, Tran JT, Brush RS, Saadi A, Rahman AK, Yu M, Yasumura D, Matthes MT, Ahern K, Yang H, LaVail MM, Mandal MN. Ceramide signaling in retinal degeneration. Adv Exp Med Biol. 2012; 723:553–558. [PubMed: 22183377]

Dowler S, Kular G, Alessi DR. Protein lipid overlay assay. Sci STKE. 2002; 16

Fabrias G, Munoz-Olaya J, Cingolani F, Signorelli P, Casas J, Gagliostro V, Ghidoni R. Dihydroceramide desaturase and dihydrosphingolipids: debutant players in the sphingolipid arena. Prog Lipid Res. 2012; 51:82–94. [PubMed: 22200621]

Folch J, Lees M, Sloane Stanley GH. A simple method for the isolation and purification of total lipids from animal tissues. J Biol Chem. 1957; 226:497–509. [PubMed: 13428781]

Ford DA, Monda JK, Brush RS, Anderson RE, Richards MJ, Fliesler SJ. Lipidomic analysis of the retina in a rat model of Smith-Lemli-Opitz syndrome: alterations in docosahexaenoic acid content of phospholipid molecular species. J Neurochem. 2008; 105:1032–1047. [PubMed: 18182048]

Fox TE, Han X, Kelly S, Merrill AH 2nd, Martin RE, Anderson RE, Gardner TW, Kester M. Diabetes alters sphingolipid metabolism in the retina: a potential mechanism of cell death in diabetic retinopathy. Diabetes. 2006; 55:3573–3580. [PubMed: 17130506]

Garanto, A. CERKL, generació d'un model knockout de retinosi pigmentària iestudis funcionals, Genetics. Universitat de Barcelona; Barcelona: 2011.

Garanto A, Riera M, Pomares E, Permanyer J, de Castro-Miro M, Sava F, Abril JF, Marfany G, Gonzalez-Duarte R. High transcriptional complexity of the retinitis pigmentosa CERKL gene in human and mouse. Invest Ophthalmol Vis Sci. 2011; 52:5202–5214. [PubMed: 21508105]

Garanto A, Vicente-Tejedor J, Riera M, de la Villa P, Gonzalez-Duarte R, Blanco R, Marfany G. Targeted knockdown of Cerkl, a retinal dystrophy gene, causes mild affectation of the retinal ganglion cell layer. Biochim Biophys Acta. 2012; 1822:1258–1269. [PubMed: 22549043]

German OL, Miranda GE, Abrahan CE, Rotstein NP. Ceramide is a mediator of apoptosis in retina photoreceptors. Invest Ophthalmol Vis Sci. 2006; 47:1658–1668. [PubMed: 16565407]

Graf C, Niwa S, Muller M, Kinzel B, Bornancin F. Wild-type levels of ceramide and ceramide-1-phosphate in the retina of ceramide kinase-like-deficient mice. Biochem Biophys Res Commun. 2008; 373:159–163. [PubMed: 18555012]

Hannun YA, Obeid LM. Principles of bioactive lipid signalling: lessons from sphingolipids. Nat Rev Mol Cell Biol. 2008; 9:139–150. [PubMed: 18216770]

Hirabayashi Y. A world of sphingolipids and glycolipids in the brain – novel functions of simple lipids modified with glucose. Proc Jpn Acad Ser B Phys Biol Sci. 2012; 88:129–143.

Inagaki Y, Mitsutake S, Igarashi Y. Identification of a nuclear localization signal in the retinitis pigmentosa-mutated RP26 protein, ceramide kinase-like protein. Biochem Biophys Res Commun. 2006; 343:982–987. [PubMed: 16581028]

Kitatani K, Idkowiak-Baldys J, Hannun YA. The sphingolipid salvage pathway in ceramide metabolism and signaling. Cell Signal. 2008; 20:1010–1018. [PubMed: 18191382]

Lahiri S, Futerman AH. The metabolism and function of sphingolipids and glycosphingolipids. Cell Mol Life Sci. 2007; 64:2270–2284. [PubMed: 17558466]

Littink KW, Koenekoop RK, van den Born LI, Collin RW, Moruz L, Veltman JA, Roosing S, Zonneveld MN, Omar A, Darvish M, Lopez I, Kroes HY, van Genderen MM, Hoyng CB, Rohrschneider K, van Schooneveld MJ, Cremers FP, den Hollander AI. Homozygosity mapping in patients with cone–rod dystrophy: novel mutations and clinical characterizations. Invest Ophthalmol Vis Sci. 2010; 51:5943–5951. [PubMed: 20554613]

Mencarelli, C.; Martinez-Martinez, P. Ceramide function in the brain: when a slight tilt is enough. Cell Mol Life Sci. 2012. http://dx.doi.org/10.1007/s00018-012-1038-x (online June 2012)

Merrill AH Jr, Sullards MC, Allegood JC, Kelly S, Wang E. Sphingolipidomics: high-throughput, structure-specific, and quantitative analysis of sphingolipids by liquid chromatography tandem mass spectrometry. Methods. 2005; 36:207–224. [PubMed: 15894491]

Miranda GE, Abrahan CE, Agnolazza DL, Politi LE, Rotstein NP. Ceramide-1-phosphate, a new mediator of development and survival in retina photoreceptors. Invest Ophthalmol Vis Sci. 2011; 52:6580–6588. [PubMed: 21724910]

Miranda GE, Abrahan CE, Politi LE, Rotstein NP. Sphingosine-1-phosphate is a key regulator of proliferation and differentiation in retina photoreceptors. Invest Ophthalmol Vis Sci. 2009; 50:4416–4428. [PubMed: 19357361]

Nevet MJ, Vekslin S, Dizhoor AM, Olshevskaya EV, Tidhar R, Futerman AH, Ben-Yosef T. Ceramide kinase-like (CERKL) interacts with neuronal calcium sensor proteins in the retina in a cation-dependent manner. Invest Ophthalmol Vis Sci. 2012; 53:4565–4574. [PubMed: 22678504]

Pomares E, Marfany G, Brion MJ, Carracedo A, Gonzalez-Duarte R. Novel high-throughput SNP genotyping cosegregation analysis for genetic diagnosis of autosomal recessive retinitis pigmentosa and Leber congenital amaurosis. Hum Mutat. 2007; 28:511–516. [PubMed: 17279538]

Rotstein NP, Miranda GE, Abrahan CE, German OL. Regulating survival and development in the retina: key roles for simple sphingolipids. J Lipid Res. 2010; 51:1247–1262. [PubMed: 20100817]

Rovina P, Schanzer A, Graf C, Mechtcheriakova D, Jaritz M, Bornancin F. Subcellular localization of ceramide kinase and ceramide kinase-like protein requires interplay of their Pleckstrin Homology domain-containing N-terminal regions together with C-terminal domains. Biochim Biophys Acta. 2009; 1791:1023–1030. [PubMed: 19501188]

Ruiz A, Winston A, Lim YH, Gilbert BA, Rando RR, Bok D. Molecular and biochemical characterization of lecithin retinol acyltransferase. J Biol Chem. 1999; 274:3834–3841. [PubMed: 9920938]

Sanvicens N, Cotter TG. Ceramide is the key mediator of oxidative stress-induced apoptosis in retinal photoreceptor cells. J Neurochem. 2006; 98:1432–1444. [PubMed: 16923157]

Strettoi E, Gargini C, Novelli E, Sala G, Piano I, Gasco P, Ghidoni R. Inhibition of ceramide biosynthesis preserves photoreceptor structure and function in a mouse model of retinitis pigmentosa. Proc Natl Acad Sci U S A. 2010; 107:18706–18711. [PubMed: 20937879]

Tang Z, Wang Z, Wang Z, Ke T, Wang QK, Liu M. Novel compound heterozygous mutations in CERKL cause autosomal recessive retinitis pigmentosa in a nonconsanguineous Chinese family. Arch Ophthalmol. 2009; 127:1077–1078. [PubMed: 19667359]

Tuson M, Garanto A, Gonzalez-Duarte R, Marfany G. Overexpression of CERKL, a gene responsible for retinitis pigmentosa in humans, protects cells from apoptosis induced by oxidative stress. Mol Vis. 2009; 15:168–180. [PubMed: 19158957]

Tuson M, Marfany G, Gonzalez-Duarte R. Mutation of CERKL, a novel human ceramide kinase gene, causes autosomal recessive retinitis pigmentosa (RP26). Am J Hum Genet. 2004; 74:128–138. [PubMed: 14681825]

Vekslin S, Ben-Yosef T. Spatiotemporal expression pattern of ceramide kinase-like in the mouse retina. Mol Vis. 2011; 16:2539–2549. [PubMed: 21151604]

Abbreviations

SPL	Sphingolipid
DhSPL	Dihydrosphingolipid
CER	Ceramide
C1P	Ceramide-1-Phosphate
SPH	Sphingosine
S1P	Sphingosine-1-Phosphate
DhCER	Dihydroceramide
MHCer	Monohexosyl Ceramide
GlcCer	Glucosyl Ceramide
GalCer	Galactosyl Ceramide
LacCer	Lactosyl Ceramide
SM	Sphingomyelin
DhSM	Dihydrosphingomyelin
GlycoSPL	Glycosphingolipid
PL	Phospholipid
NL	Neutral lipid
PS	Phosphatidylserine
PC	Phosphatidylcholine
PI	Phosphatidylinositol
PE	Phosphatidylethanolamine
PA	Phosphatidic acid
LPA	Lysophosphatidic Acid
LPC	Lysophosphatidylcholine
LPI	Lysophosphatidylinositol
LPE	Lysophosphatidylethanolamine
MAG	Monoacylglycerol

DAG	Diacylglycerol
TAG	Triacylglycerol
CE	Cholesterol ester
SMase	Sphingomyelinase
CERK	Ceramide Kinase
CERKL	Ceramide Kinase-Like
RP	Retinitis Pigmentosa
CRD	Cone–Rod Dystrophy
STGD1	Stargardt disease 1
STGD3	Stargardt disease 3
LCA	Leber Congenital Amaurosis
FA	Fatty Acid
FFA	Free Fatty Acid
FFAC	Free Fatty Acid Chain *n* (*n* indicating the length of the carbon chain)
VLCFFA	Very Long Chain Free Fatty Acid
PUFA	Polyunsaturated Fatty Acid
VLCPUFA	Very Long Chain Polyunsaturated Fatty Acid
VLCCER	Very Long Chain Ceramide
VLCSPL	Very Long Chain Sphingolipid
DHA	Docosahexaenoic Acid
DTPA	Diethylene Triamine Pentaacetic Acid
UPLC-TOF	Ultra Performance Liquid Chromatography-Time of Flight

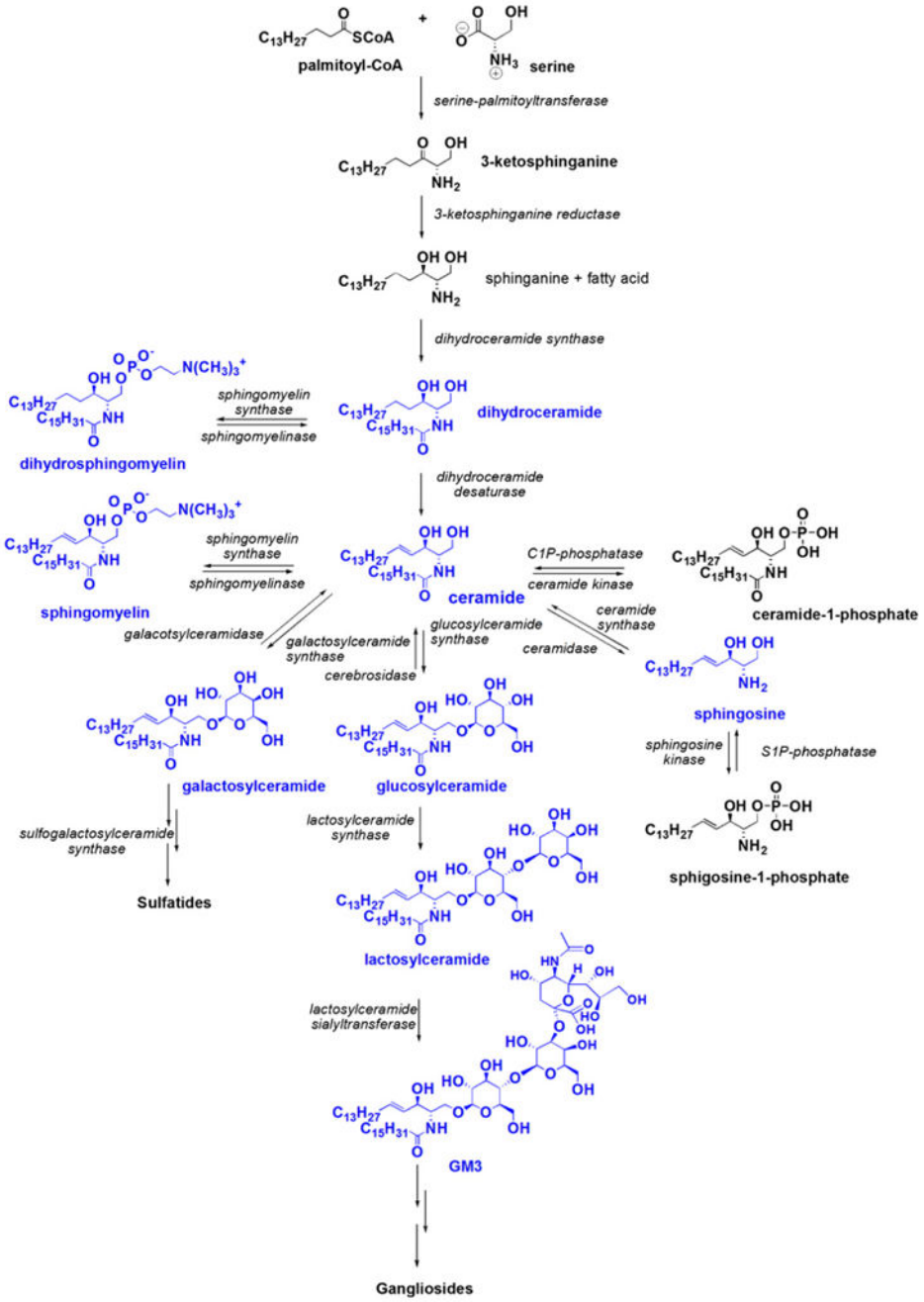

Fig. 1.

Diagram of the sphingolipid metabolism. The de novo synthesis pathway starts at the endoplasmic reticulum by the condensation of palmitate and serine to produce 3-ketosphinganine, which is then reduced to sphinganine, and converted to DhCER by the addition of a fatty acid. CER is the core molecule of SPL metabolism and is formed by the desaturation of DhCER. CER is the precursor of SPH, C1P, and a collection of complex SPLs: SM, GlcCer, GalCer and its derivatives. The SPL groups analyzed and quantified in

this work are depicted in blue. (For interpretation of the references to colour in this figure legend, the reader is referred to the web version of this article.)

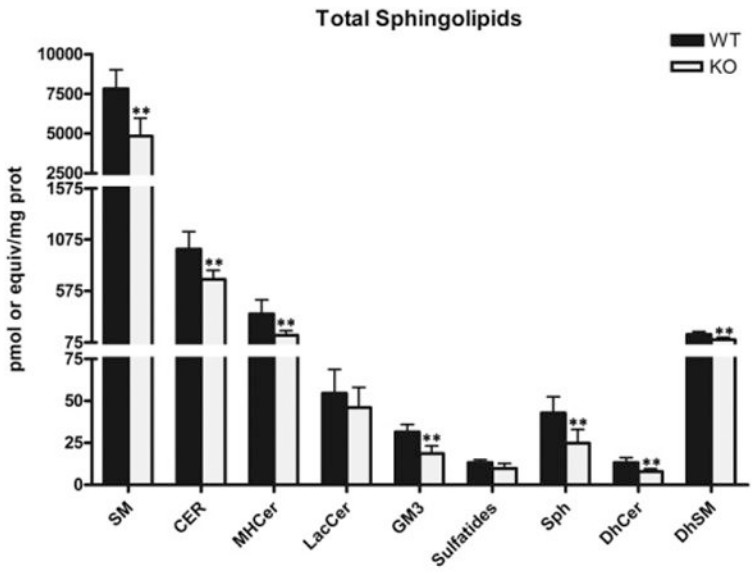

Fig. 2.

Sphingolipid quantification in WT and KO retinas. The SPL content was resolved and quantified from P60 retinas of 6 WT and *Cerkl* −/− retinas. Note that the y axis (pmol/mg prot) is discontinuous, divided in three segments that overall encompass 4 orders of magnitude. Decreased levels of several SPLs were observed in the KO retinas (**$p < 0.01$, Mann–Whitney test). Note that LacCer and GM3 values were quantified using MHCer standards, whereas CER standards were used for sulfatides.

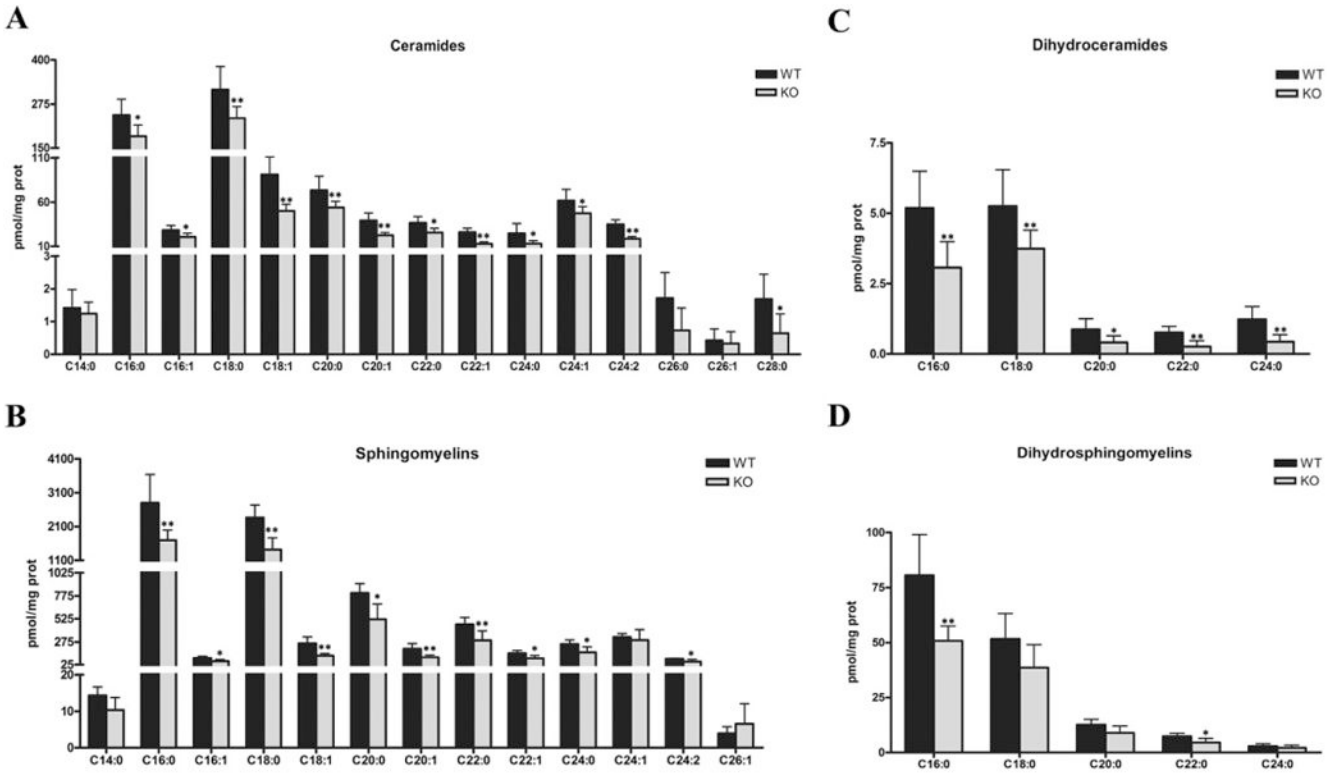

Fig. 3.

Retinal ceramide, sphingomyelin, dihydroceramide, and dihydrosphingomyelin species in WT and *Cerkl* −/− mice. (A) Ceramide species quantification. (B) Sphingomyelin species quantification. (C) Dihydroceramide (the CER precursor) species quantification. (D) Dihydrosphingomyelin (produced from DhCER by the addition of phosphocholine group) species quantification. Note that the *y* axis (pmol/mg prot) is discontinuous in (A) and (B), divided in three segments that overall encompass 3 or 4 orders of magnitude. Significant differences were observed (*$p < 0.05$, **$p < 0.01$, Mann–Whitney test).

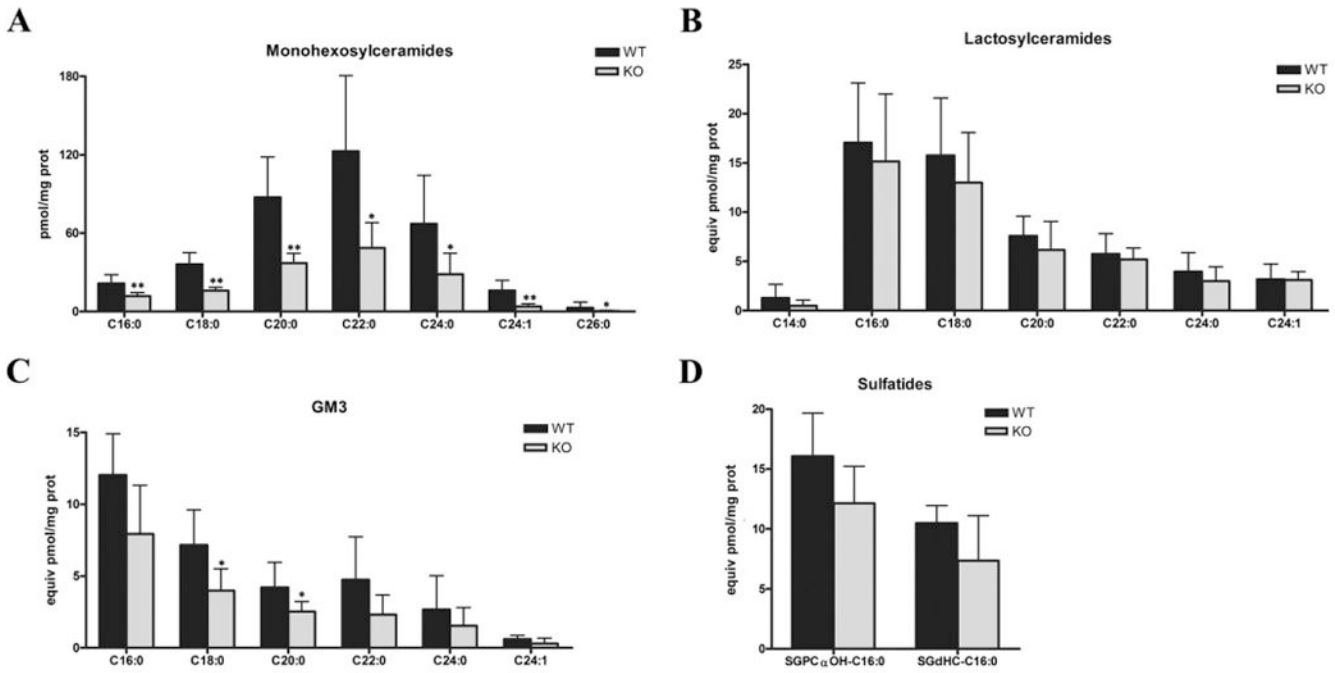

Fig. 4.

Glycolipid species determination and quantification in WT and *Cerkl* −/− retinas. (A) Monohexosyl ceramide (glucosyl- and galactosylceramide) species. GlcCer and GalCer are directly synthesized from CER. (B) Lactosyl ceramide (derived from GlcCer) species determination and quantification. (C) GM3 species analysis and quantification. GM3 is produced from LacCer by the addition of a sialic acid. (D) Sulfatide (produced from GalCer) species determination and quantification. Significant differences were observed in Glc/GalCer, LacCer species, and GM3 (**$p < 0.01$, Mann–Whitney test). Note that LacCer and GM3 values were quantified using MHCer standards, whereas CER standards were used for sulfatides.

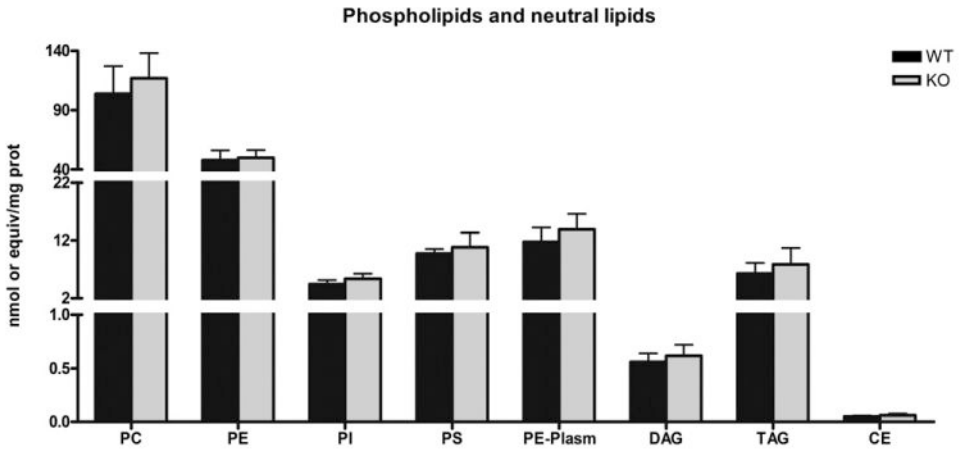

Fig. 5.

Retinal phospholipid and neutral lipid content in WT and *Cerkl* −/− retinas. DAG, TAG and CE levels were quantified using PC standards whereas PI was referred to (C17:0/C17:0-PE). Note that the *y* axis (nmol/mg prot) is discontinuous, divided in three segments that overall encompass 3 orders of magnitude. No significant changes in any of these lipid groups were observed in WT and KO retinas.

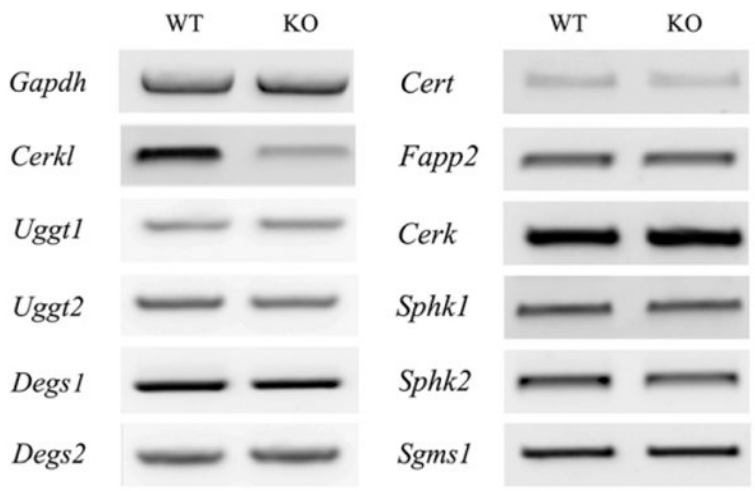

Fig. 6.

Semiquantitative expression analysis of SPL genes. Transcription levels of the genes involved in the synthesis of CER, SM, GlcCer and GalCer, as well as SPL kinases and transporters were analyzed on WT and KO retinas. No differences were observed. *Gapdh* and *Cerkl* were used for sample normalization and control, respectively.

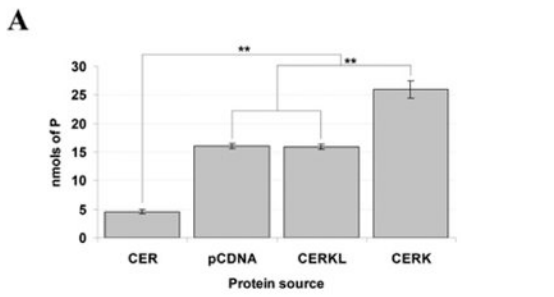

B

Group	Lipid-containing micelles
Group 0	Empty micelles
Group 1	GlcCer, GalCer, LacCer, GM1
Group 2	SPH, SM
Group 3	PS, PA, PC, PI, PE
Group 4	LPA, LPC, LPI, LPE
Group 5	Cholesterol, cholesterol esters
Group 6	MAG, DAG, TAG
Group 7	FFAC12, FFAC14, FFAC16, FFAC18
Group 8	FFAC20, FFAC22, FFAC24

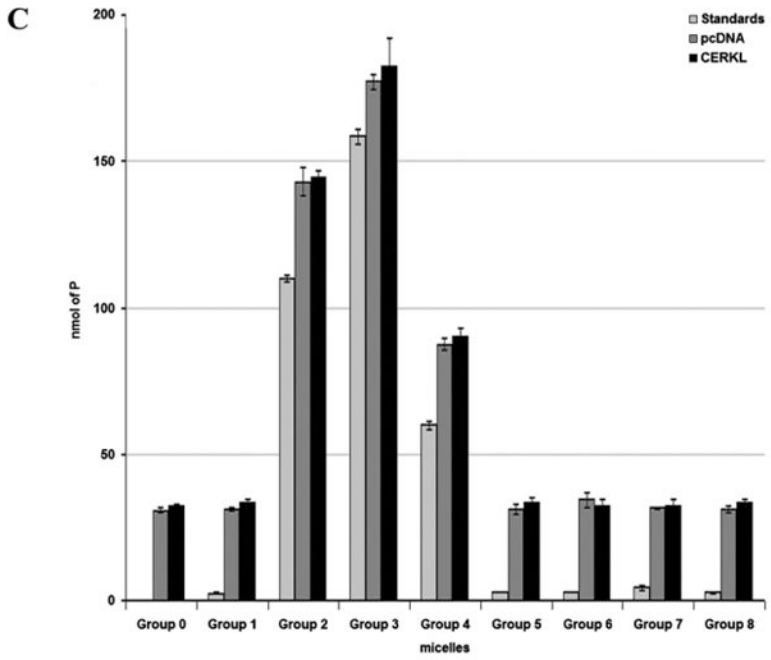

Fig. 7.

CERKL kinase activity assessment. (A) Validation of the sensitivity of the phosphorus incorporation assay using ceramide-containing micelles mixed with protein lysates of cells overexpressing either CERKL or CERK (positive control). CERKL did not phosphorylate CERs under standard conditions. (B) Custom-made synthetic micelles containing several commercial lipids and SPLs combined according to their structure and similarity. Group 0 corresponded to the negative control with empty micelles. (C) Phosphorus incorporation assays using the micelles listed in (B) together with, either no protein lysate (light gray), empty vector protein lysate (medium gray) or CERKL-transfected cell lysate (dark gray). No significant differences were observed at incorporated phosphorus levels (Mann–Whitney test).

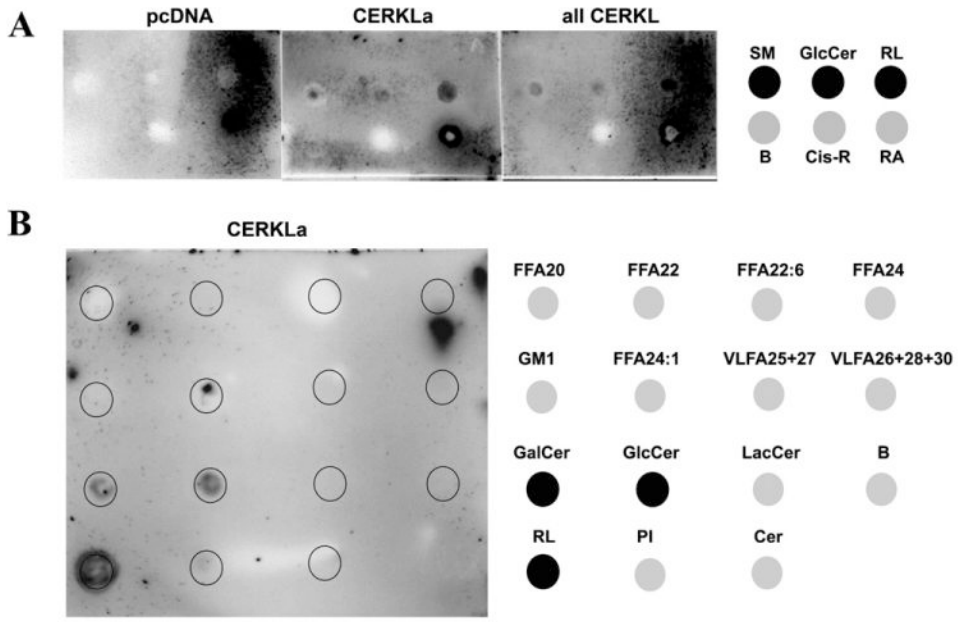

Fig. 8.

Protein–lipid overlay analysis. One representative replicate (of at least three) is shown in this figure. (A) Membranes spotted with bovine retinal lipids (RL) (positive control), SM, GlcCer, cis-retinol (cis-R) and retinoic acid (RA) were incubated with lysates of HEK293T cells transfected with either the empty vector (pcDNA), CERKLa (considered the reference CERKL transcript isoform) or 4 CERKL isoforms co-transfection (CERKLa, b, c and d). B indicates Blank (negative control). Immunodetection showed CERKL binding with RL, SM and GlcCer. (B) Free fatty acids (FFA), very long chain fatty acids (VLCFA), phosphatidylinositol mixture (PI) and other SPLs were also tested. Positive signal was only detected in RL (positive control), GlcCer and GalCer. The graphics on the right show the lipid distribution on the membranes.

Table 1

RT-PCR oligonucleotide sequences.

Gene	Forward 5′ → 3′	Reverse 5′ → 3′
Gapdh	TGAAGGTCGGAGTCAACGGATTTGG	CATGTAGGCCATGAGGTCCACCAC
Cerkl	CTGACTGTGGTGGTCACTGG	GAACCTCTGATGCAGCTTCC
Cert	CGTAGACATGGCTCAATGGTG	ACTCTTCCTCATTAATCAGACTG
Fapp2	TGGATTGCAGCATCTCCAGTG	AGACCTCTCTTCAGCCACAAG
Cerk	GCTTCCATCACTACGGAGATC	CTGAGAAATCATACCGGACGAG
Sphk1	GCATAATGGGAACGGCCAFACTG	GTTCTGGTACCACAGTCCAATG
Sphk2	GGCAGCGCTGTATGGACCAC	GCACTGCACCCAGTGTGAATC
Uggt1	TGATGAAGGACATTAGTCAGAAC	TCTCGGCGATGCTAATCAACTC
Uggt2	CATCGTATACTCACTGTGGATG	CAGCAATAATCCACAGAGTGAC
Ugt8a	GAGCTGGTGTCAAGTATCTGTC	GGGCTCCGTCATGGCGAAG
Sgms1	CACGCTGTACCTGTATCGGTG	ATGGTAAGATCGAGGTACAATTC
Sgms2	GGAACTTTATACCTGTATCGCTG	GCAAGGAATTGAGCCTTGCAC
Degs1	GCGTGTCCCGAGAGGAGTTC	GCAGAAGAACCAGCCCTCG
Degs2	AATGGTACTGGTTCAGGTGCTG	GCTGCTGCCTAGAAGGTAGAC